Molecular Crystals and Liquid Crystals

ISSN: 1542-1406 (Print) 1563-5287 (Online) Journal homepage: http://www.tandfonline.com/loi/gmcl20

Growth of Inorganic Solid Nanorods by Hot Filament Chemical Vapor Deposition Technique

M. Ghoranneviss, A. Salar Elahi & R. Bakhshkandi

To cite this article: M. Ghoranneviss, A. Salar Elahi & R. Bakhshkandi (2015) Growth of Inorganic Solid Nanorods by Hot Filament Chemical Vapor Deposition Technique, Molecular Crystals and Liquid Crystals, 609:1, 228-234, DOI: 10.1080/15421406.2014.956401

To link to this article: http://dx.doi.org/10.1080/15421406.2014.956401

Published online: 11 Apr 2015.

Mol. Cryst. Liq. Cryst., Vol. 609: pp. 228–234, 2015

ISSN: 1542-1406 print/1563-5287 online
DOI: 10.1080/15421406.2014.956401

Taylor & Francis
Taylor & Francis Group

Growth of Inorganic Solid Nanorods by Hot Filament Chemical Vapor Deposition Technique

M. GHORANNEVISS, A. SALAR ELAHI,* AND R. BAKHSHKANDI

Plasma Physics Research Center, Science and Research Branch, Islamic Azad University, Tehran, Iran

The aim of this research is to demonstrate the growth of titanium dioxide nanorods. In our testing, growth of nanorods was achieved using the hot filament chemical vapor deposition method. We studied the effects of temperature and time on the growth of nanorods. We also investigated the effect of Co catalyst on the growth of nanorods so that we could measure the Ti content at different times and temperatures. Our samples were studied using scanning electron microscopy, Raman spectroscopy, energy-dispersive x-ray spectroscopy, dot mapping, and x-ray diffraction. Diameter and length of nanorods were 262.07 nm and 719.41–821.38 nm, respectively. Raman spectroscopy was indicative of two peaks (anatase and rutile). The anatase peaks were 650°C, 490, 509, 558, 613, 787 cm^{-1}; and the rutile peak was 435 cm^{-1}. Results show that titanium dioxide nanorods had their best growth and penetration when Co was used as a catalyst at a time of 30 min and a temperature of 650°C.

Keywords HFCVD; nano-materials; nanorods; titanium dioxide

1. Introduction

Nanoscaled materials are of great interest for their unique structure and properties. Nanowires and nanorods of various compositions have been synthesized for potential use as quantum wires in nano-devices as photo catalysts, mesoporous structures, and for other functional applications [1]. Nano-crystalline titania is an important oxide ceramic material that has shown a lot of promise in various applications such as photo-catalysis, solar cells, oil and water purification, nitrogen fixation, and gas sensors [2].

Titanium dioxide (TiO_2) is a fascinating class of inorganic solids used in a wide range of common and high technique applications because of its moderate price, chemical stability, non-toxicity, biocompatibility, very high reflectivity of light, efficient photo-catalysis, and surface reactivity. These properties can be controlled by TiO_2 crystal structure, crystallite size, size distribution, and morphology. Crystalline TiO_2 exists in three polymorphic forms: anatase (tetragonal, c/a $>$ 1), rutile (tetragonal, c/a $<$ 1), and brookite (orthorhombic). Rutile is a thermodynamically stable phase (generally in 600–1855°C), whereas anatase and brookite are metastable and are readily transformed to rutile when heated. The phase

*Address correspondence to A. Salar Elahi, Plasma Physics Research Center, Science and Research Branch, Islamic Azad University, Tehran, Iran. E-mail: Salari_phy@yahoo.com

Color versions of one or more of the figures in the article can be found online at www.tandfonline.com/gmcl.

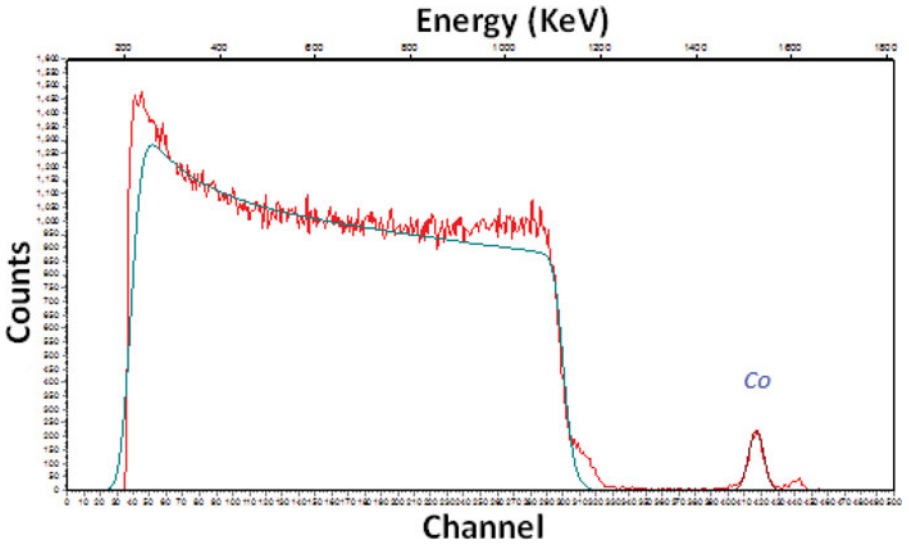

Figure 1. The RBS pattern at 2.5 min.

change from anatase to rutile has been reported to occur at different temperature ranges from 600°C to 1100°C, depending on the preparation conditions, particle size, and the presence of impurities. Anatase TiO_2 has been widely studied due to its tremendous technological importance in various applications. Anatase TiO_2 has the (101) plane, which is the most exposed face in nanocrystals. For rutile TiO_2, the (110) face has been shown to be the exposed plane [3].

A large number of publications has been focused on the production of nanostructured TiO_2 using different techniques such as vapor–liquid–solid (VLS) [4], chemical vapor deposition (CVD) [5], plasma electrolytic deposition [6], solution–liquid–solid (SLS) [7], laser-assisted catalytic growth [8], sol-gel [9], surfactant-directed [10], electron beam lithography [11], solvothermal [12], and the filling of templates with colloidal oxide particles [13,14].

Nano-crystalline TiO_2 has been widely studied during the past few years because of its many applications such as electrodes for electrochemical detection [15], gas sensors [16], photo-catalysis [17,18], dye-sensitization for solar cells [18,19], and solar water splitting for hydrogen production [20].

2. Experimental

In this project, we first cut a silicon wafer with an original diameter of 20 cm into 1 × 1 cm pieces, clean the pieces using acetone (C_3H_6O), etanol (C_2H_6O), and DI water in an ultrasonic cleaner, and then deposited layer of Co (as a catalyst) on the silicon substrate using a plasma-enhanced chemical vapor deposition (PECVD) device. Thickness of Co layer is measured using the Rutherford Backscattering (RBS) device. Sample surfaces will be pictured topographically using atomic force microscopy (AFM). In this work, before the growth of TiO_2 nanorods begins in each test, operation is conducted. Gases used for etching are H_2 and NH_3, which are injected into the reaction chamber, ionized into free radicals by a heated filament, and are brought in contact with surfaces. These conditions will result in the perforation of surfaces and creation of the needed sites over the catalyst film. Eventually

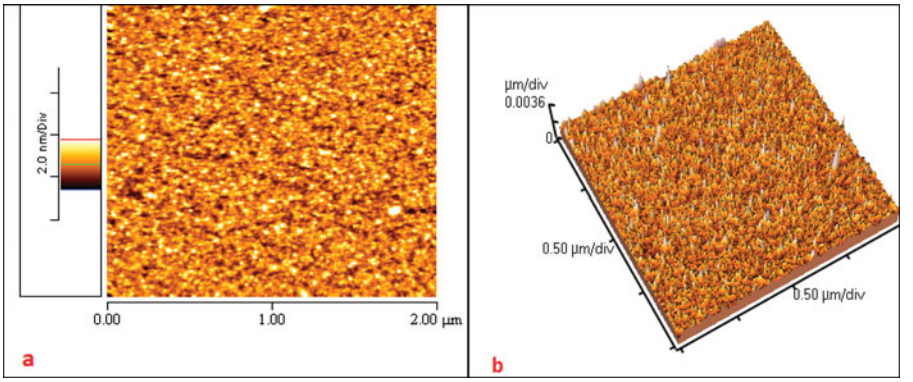

Figure 2. AFM image of the Co catalyst layer at 2.5 min before etching.

and after the etching, AFM analysis is conducted and coarseness of the surfaces before and after etching is measured and recorded. After the surfaces are primed and the catalyst layer is set, TiO_2 nanostructures are cultivated using a hot filament chemical vapor deposition (HFCVD) device. The silicon substrate (which is coated with Co catalyst) is placed upon the heater surface and the system is sealed so that the inside can be vacuumed using rotary pump and diffusion. An initial vacuum of 10-3 torr is achieved before the samples are etched, which is done before the outset of the actual growth stage. Here NH_3 and H_2 gases are used for etching in the manner explained below. H_2 with a flow of 48.4 sccm and NH_3 with a flow of 48.4 sccm are injected into the chamber. Pressure is set to 5 torr and the temperature is adjusted at 567°C. A voltage of 5 V and a current of 13.5 A are applied. NH_3 and H_2 molecules hit the heated filament and the catalyst surface and the etching is thus achieved. This operation takes 10 min and is followed by the actual growth stage. At this stage, titanium tetra-isopropoxide (TTIP) is used as a precursor and Ar is used as a carrier gas and extenuator. After etching is completed, Ar with a flow of 63.2 sccm is injected into the TTIP chamber. It comes in contact with TTIP and is heated to 650°C along with other vapors. It is then mixed with NH_3 vapors with a flow of 63.2 sccm and the mixture is injected into the reaction chamber of HFCVD device. After the completion of growth stage, Ar/NH_3 and TTIP gas flows are stopped and the filament and the system as a whole

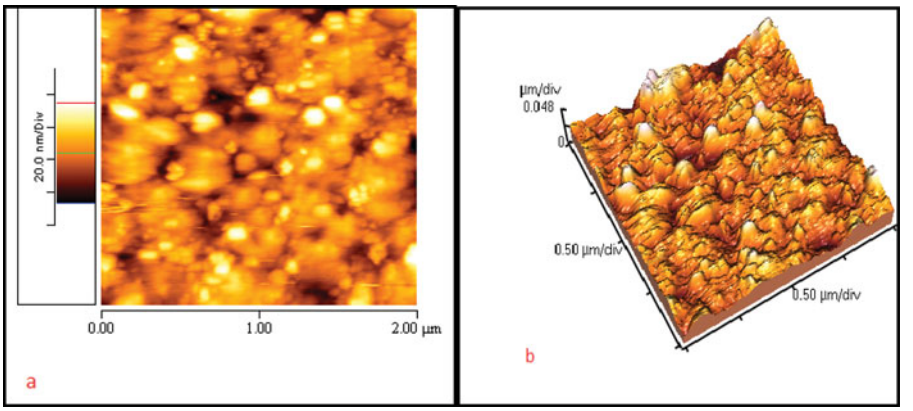

Figure 3. AFM image of the Co catalyst layer at 10 min after etching.

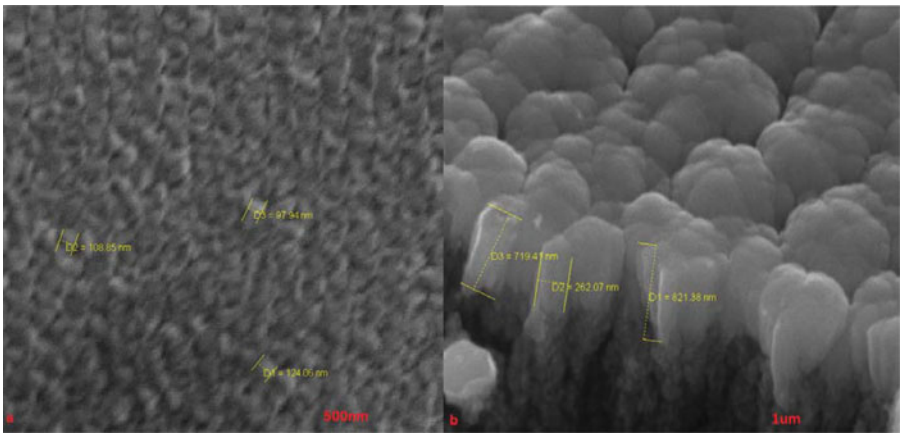

Figure 4. SEM image of grown TiO_2 nanorods at temperatures of (a) 567°C, and (b) 650°C.

is left to cool. Eventually after the device is cooled enough, the vacuum seal is broken, the sample is taken out from the chamber, and transferred to analysis center to undergo scanning electron microscopy (SEM), Raman spectroscopy, energy-dispersive x-ray (EDX) spectroscopy, and dot mapping.

3. Results

Figure 1 shows the RBS. It is seen that for a deposition time of 2.5 min, thickness of the Co catalyst layer is equal to 6.57 nm. Figure 2 shows the result of AFM for the pre-etching situation. This was obtained at 2.5 min and a voltage of 1 kV and under Ar gas with a flow of 79.3 sccm. Figure 2b is the AFM of Co atoms for a 0.5 × 0.5 μm/div array. Average coarseness of Co layer is 0.3090 nm. Figure 3 shows the AFM result for Co catalyst layer at 10 min and under H_2 and NH_3 gas (mixed) with a flow of 48.4 sccm at 567°C. This

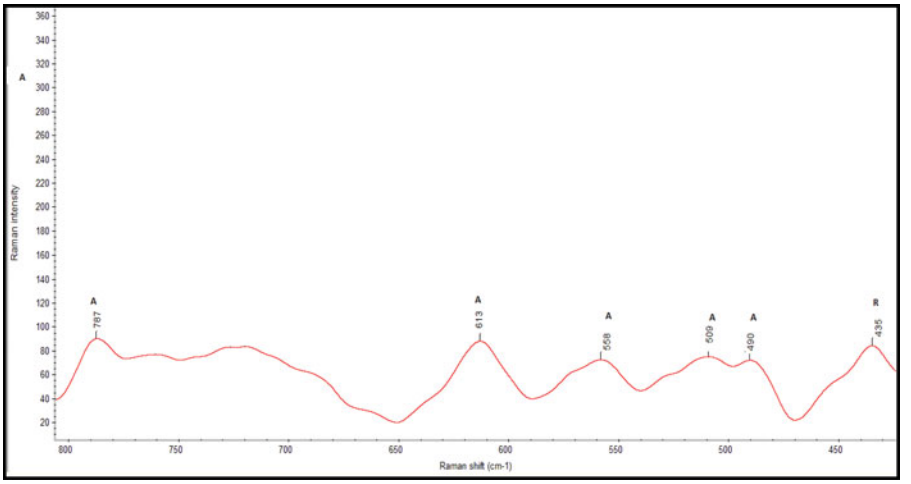

Figure 5. Raman spectra of TiO_2 at 650°C.

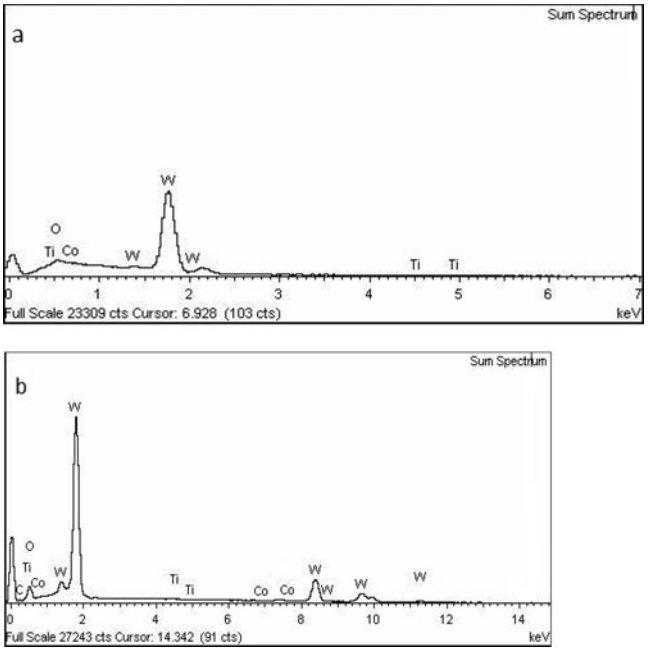

Figure 6. EDX analysis shows the surface at (a) 567°C and 15 min, and (b) 650°C and 30 min.

result is for a post-etching situation. Figure 3a shows the two-dimensional topography of the Co catalyst layer, which has an average roughness of 7.860 nm, and Fig. 3b is a three-dimensional picture of 0.5 × 0.5 μm/div array. Figure 4 shows the SEM results. Figure 4a shows the result at 15 min and a pressure of 1 torr, Ar and NH_3 flow being 63.2 sccm; voltage, current, and temperature being set at 5V, 13A, and 567°C respectively. At this temperature the Co surface is graying, with measured sizes of grains being 124.06,

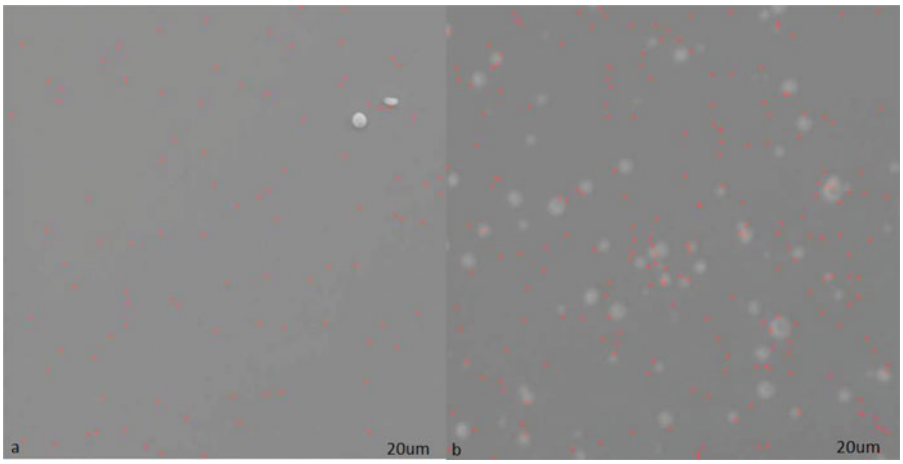

Figure 7. Dot mapping image shows the surface at 15 min and 30 min at temperatures of 567°C and 650°C.

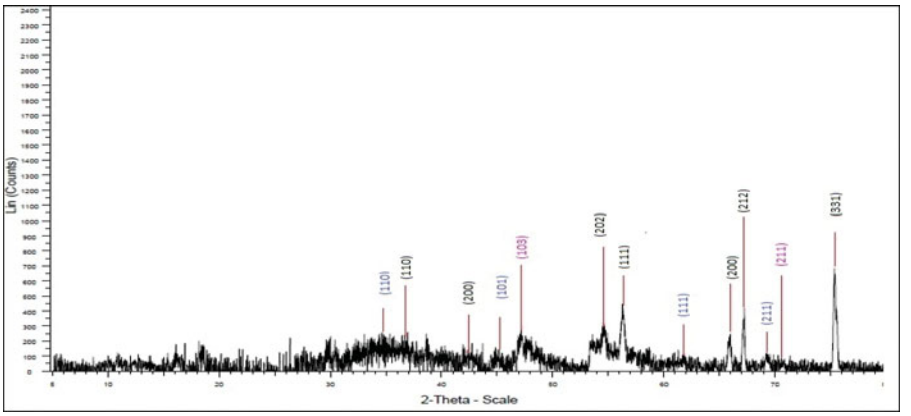

Figure 8. XRD of the TiO_2 nanorods at 30 min and a temperature of 650°C.

97.94, and 108.85 nm. Figure 4b depicts the situation where, at a time of 30 min, the pressure and temperature are 1 torr and 650°C respectively. Ar and NH_3 gas flow is 63.2 sccm and the current is set at 13.3 A. The SEM picture has a resolution of 1 um and shows that TiO_2 nanorods have a length of 821.38 nm and a diameter of 262.06 nm. Figure 5a shows the Raman spectrometry at 30 min and 650°C. At a temperature of 650°C, 490, 509, 558, 613, 787 cm^{-1} peaks are generated by the anatase phase whereas 435 cm^{-1} peaks are generated by the rutile phase. Figure 6a shows the results of EDX analysis at 15 min and 567°C. Here signals are from Co, O, and Ti. Weight percentages of Co and O are 0.5 and 17.38 respectively. Weight percentage of Ti on Co catalyst is 0.2%. Figure 6b shows signals related to the O, Co, Ti, and C found in TiO_2 nanorods. This is the situation at 30 min and at a temperature of 650°C. Weight percentages of C, O, and Co are 3.54, 14.9, and 0.05 respectively. Weigh percentage of Ti under these conditions is 0.13. Figure 7 shows the results of dot mapping analysis at 567°C and 650°C. Figure 7a shows the sample surface at 15 min time and at a temperature of 567°C. Red dots on the surface represent Ti, the resolution of the image being 20 um. Figure 7b shows the surface at 30 min time and at a temperature of 650°C. It can be seen that the amount of Ti increases with time and temperature. We can surmise from d (Lattice points distance) that Ti has penetrated deep unto the nanorods. Figure 8 shows the results of X-ray diffraction (XRD) analysis. The analysis was done at 0.2 steps; 34.37, 45.3, 51.9, and 69.27 show (110), (101), (111), and (211) surfaces respectively for the rutile phase; 47.01 and 71.19 show (103) and (211) surfaces respectively for the anatase phase; 56.6 and 65.8 show (111) and (200) Co surfaces respectively; 1.24 shows (331) silicon surface; and 54.8, 67.75, 42.4, 20.8, and 36.5 show (202), (212), (200), (100), and (331) SiO_2 surfaces respectively.

4. Conclusions

Using the CVD method and the heated filament, we were able to manufacture TiO_2 nanorods. Considering the picture of SEM results, at a temperature of 650°C these nanorods have a diameter of 821.38 nm and a length of 262.07 nm. The XRD analysis results showed that TiO_2 nanorods are crystallized either as anatase or rutile. The EDX analysis and dot mapping results showed that weight percentage and permeation of Ti onto the surfaces

increased with time and temperature. Also, length and diameter of nanorods improved with time and temperature.

References

[1] Pradhan, S. K., Reucroft, P. J., Yang, F., & Dozier, A. (2003). *J. Crystal Growth*, *256*, 83–88.
[2] Md, I. A., & Bhattacharya, S. S. (2008). *J. Phys. D: Appl. Phys.*, *41*, 155313, doi:10.1088/0022-3727/41/15/155313.
[3] SadeghzadehAttar, A. *et al.* (2008). *J. Mater. Sci.*, *43*, 5924–5929.
[4] Wu, Y., & Yang, P. (2001). *J. Am. Chem. Soc.*, *123*, 3165–3166.
[5] Pradhan, S. K., Reucroft, P. J., Yang, F., & Dozier, A. (2003). *J. Crystal Growth*, *256*, 83–88.
[6] Markowitz, P. D., Zach, M., Gibbons, P. C., Penner, R. M., & Buhro, W. E. (2001). *J. Am. Chem. Soc.*, *123*, 4502–4511.
[7] Morales, A. M., & Lieber, C. M. (1998). *Science*, *279*, 208–211.
[8] Sugimoto, T., Zhou, X., & Muramatsu, A. (2003). *J. Coll. Interface Sci.*, *259*, 53–61.
[9] Cozzoli, P. D., Kornowski, A., & Weller, H. (2003). *J. Am. Chem. Soc.*, *125*, 14539–14548.
[10] Zhao, X.-M., Xia, Y., & Whitesides, G. M. (1997). *J. Mater. Chem.*, *7*, 1069–1074.
[11] Kim, C.-S., Moon, B. K., Park, J.-H., Choi, B.-C., & Seo, H.-J. (2003). *J. Crystal Growth*, *257*, 309–315.
[12] Lakshmi, B. B., Dorhout, P. K., & Martin, C. R. (1997). *Chem. Mater.*, *9*, 857–862.
[13] Zhang, M., Bandos, Y., & Wada, K. (2001). *J. Mater. Sci. Lett.*, *20*, 167–170.
[14] Wei, M., Qi, Z., Ichihara, M., Honma, I., & Zhou, H. (2006). *Chem. Phys. Lett.*, *424*, 316.
[15] Ruiz, A. M. *et al.* (2004). *Sensors Actuators B*, *103*, 312.
[16] Celik, E., Gokcen, Z., Ak Azem, N. F., Tanoglu, M., & Emrullahoglu, O. F. (2006). *Mater. Sci. Eng. B*, *132*, 258.
[17] Celik, E. *et al.* (2006). *Mater. Sci. Eng. B*, *129*, 193.
[18] Nazeeruddin, M. K. *et al.* (1993). *J. Am. Chem. Soc.*, *115*, 6382.
[19] Kay, A., & Grätzel, M. (1996). *Solar Energy Mater. Solar Cells*, *44*, 99.
[20] Park, J. H., Kim, S., & Bard, A. J. (2006). *Nanoletter*, *6*(1), 24.